Endoplasmic reticulum membrane tubules are distributed by microtubules in living cells using three distinct mechanisms

Clare M. Waterman-Storer and E.D. Salmon

Background: The microtubule-dependent motility of endoplasmic reticulum (ER) tubules is fundamental to the structure and function of the ER. From *in vitro* assays, three mechanisms for ER tubule motility have arisen: the 'membrane sliding mechanism' in which ER tubules slide along microtubules using microtubule motor activity; the 'microtubule movement mechanism' in which ER attaches to moving microtubules; and the 'tip attachment complex (TAC) mechanism' in which ER tubules attach to growing plus ends of microtubules.

Results: We have used multi-wavelength time-lapse epifluorescence microscopy to image the dynamic interactions between microtubules (by microinjection of X-rhodamine-labeled tubulin) and ER (by $DiOC_6(3)$ staining) in living cells to determine which mechanism contributes to the formation and motility of ER tubules in migrating cells *in vivo*. Newly forming ER tubules extended only in a microtubule plus-end direction towards the cell periphery: 31.4% by TACs and 68.6% by the membrane sliding mechanism. ER tubules, statically attached to microtubules, moved towards the cell center with microtubules through actomyosin-based retrograde flow. TACs did not change microtubule growth and shortening velocities, but reduced transitions between these states. Treatment of cells with 100 nM nocodazole to inhibit plus-end microtubule dynamics demonstrated that TAC motility required microtubule assembly dynamics, whereas membrane sliding and retrograde-flow-driven ER motility did not.

Conclusions: Both plus-end-directed membrane sliding and TAC mechanisms make significant contributions to the motility of ER towards the periphery of living cells, whereas ER removal from the lamella is powered by actomyosin-based retrograde flow of microtubules with ER attached as cargo. TACs in the ER modulate plus-end microtubule dynamics.

Address: Department of Biology, University of North Carolina, Chapel Hill, North Carolina 27599-3280, USA.

Correspondence: Clare M. Waterman-Storer
E-mail: waterman@email.unc.edu

Received: **12 March 1998**
Revised: **27 April 1998**
Accepted: **15 May 1998**

Published: **12 June 1998**

Current Biology 1998, 8:798–806
http://biomednet.com/elecref/0960982200800798

Background

Organelles such as the endoplasmic reticulum (ER), Golgi apparatus and endosomal and lysosomal compartments are comprised of anastomosing tubular membrane networks [1,2]. In living cells, tubular membrane networks of the ER and Golgi are built through a process in which a membrane tubule extends from one region of a membrane compartment, contacts and then fuses with another tubular region of the compartment to form a tubular junction between the two regions [3–7]. During membrane trafficking between the ER and Golgi, membrane tubules also extend and bud off at their distal ends from one organelle to form transport intermediates that eventually fuse with target organelles [7,8]. Thus, the extension and formation of membrane tubules is fundamentally important to organelle function as well as to the maintenance of organelle structure.

The localization of both the Golgi and the ER is dependent on microtubules (reviewed in [9,10]). At the light microscope level in fixed cells, ER tubules colocalize with single microtubules [11,12]. At the ultrastructural level in growth cones, ER tubules either associate along their length with microtubules or bind at a single point to the tips of microtubules via an electron-dense cloud [13]. The microtubule-based motors, kinesin and cytoplasmic dynein/dynactin, have been implicated in membrane trafficking in the secretory and endocytic pathways ([8,14–17], reviewed in [9,18]). The precise mechanism for microtubule-based ER tubule formation and motility in living cells is, however, unknown.

To determine how the ER forms tubular networks *in vivo*, *in vitro* assays have been developed in which dynamic membrane tubule networks form in a microtubule-dependent manner. These studies have revealed three possible mechanisms for the microtubule-dependent formation and motility of membrane tubules: the membrane sliding mechanism; the microtubule movement mechanism; and polymerization-driven microtubule tip attachment complexes

(TACs). In the membrane sliding mechanism, membrane tubules extend via a microtubule motor protein attachment between a membrane aggregate and the shaft of a microtubule. As the motor attachment slides along the microtubule, a membrane tubule is extended from the aggregate [19–22]. In the microtubule movement mechanism, a membrane attaches statically to the shaft of a moving microtubule that is sliding by motor activity either against another microtubule or along the coverslip surface [23].

Recently, we documented a third mechanism for microtubule-dependent formation of membrane tubules in interphase-arrested extracts of *Xenopus laevis* [24]. Here, ER membranes attached selectively to the growing plus ends of microtubules and extended by a polymerization-dependent mechanism that we termed a TAC. TAC-driven extension of ER tubules by plus-end polymerization was insensitive to inhibitors of microtubule motors, persisted during both growth and shortening, and did not alter the rates of growth or shortening. Subsequently, Reinsch and Karsenti [25] also observed in *Xenopus* egg extracts the movements of ER from nuclear envelopes driven by microtubule plus-end polymerization, and there is evidence that a similar phenomenon may drive the movement of phagosomes in cultured cells [26]. Similar microtubule-depolymerization-dependent movements of chromosomes or microtubule-motor-coated beads coupled to the plus ends of microtubules have also been demonstrated *in vitro* [27–29].

In this study, we use multi-wavelength time-lapse epifluorescence microscopy to observe the dynamics of ER and microtubules to determine which mechanism of membrane motility drives ER remodeling in living cells. We show that the membrane sliding and TAC mechanisms have a significant role in ER tubule formation and motility towards the cell periphery, whereas a type of microtubule movement mechanism that is driven by actomyosin-based retrograde flow of microtubules retracts pre-formed ER tubules towards the cell body.

Results

ER tubules and microtubules are closely distributed in the lamella and both undergo continuous retrograde flow

We examined ER–microtubule interactions in the lamella of migrating newt lung epithelial cells because they have a broad, flat, thin lamella that terminates at the leading edge in a ruffling lamellipodia, making them well suited to microscopy. To examine microtubule and ER dynamics in relation to one another, cells were microinjected with 2 mg/ml X-rhodamine-labeled tubulin, membranes were stained with 1.5 μg/ml $DiOC_6(3)$, and pairs of fluorescence images (within 3 seconds of each other) of microtubules and the ER were acquired at 7–10 second intervals for periods of 5–30 minutes. $DiOC_6(3)$ stained lightly the plasma membrane and more intensely the tubular reticular network of the peripheral ER [3–5,30]. Pseudocolored overlays (with microtubules red, and ER green) revealed that ER tubules were associated with microtubules along nearly their entire lengths in living cells (Figure 1), much like reports for fixed cells [11–13,31] except that ER tubules never extended beyond the ends of microtubules. This discrepancy may be due to cell-type-specific differences in retrograde flow, centripetal tension in the membrane network, or fixation artifacts.

By examining 'movies' of time-lapse series of color overlays, we noted features of the dynamic interactions between ER membrane tubules and microtubules. Many ER tubules were bound to microtubules that were undergoing a continuous slow retrograde movement towards the cell center at 0.42 ± 0.06 μm/min (Figure 1e, time 00:00–19:15, large arrows), as has been reported for either microtubules [32] or ER [30]. This movement was inhibited by 2.5 μM cytochalasin D and 25 mM 2,3-butanedione monoxime (BDM), indicating that it was dependent on actomyosin (data not shown) [30,32,33]. As retrograde flow continued, new microtubule plus ends polymerized towards the cell edge and new ER tubules extended towards the edge in association with microtubules. These extended ER tubules appeared to be under centripetal elastic tension; they were stretched smoother in profile and exhibited much less lateral Brownian motion compared with ER tubules in the more central regions of the cell. ER tubules never extended along microtubules towards the direction of cell body (that is, towards the minus ends of microtubules). When an ER tubule was associated with a shrinking microtubule, however, the tubule always retracted towards the cell body with the microtubule end, never remaining beyond it.

To determine whether retrograde flow of ER tubules required microtubules, cells were perfused with 40 μM nocodazole to induce depolymerization of microtubules. If a single, free-ended ER tubule that was extended under tension towards the leading edge was attached at its tip or along its length to a microtubule that suddenly depolymerized, the ER tubule retracted as the microtubule depolymerized. If an ER tubule was neither under apparent centripetal tension nor attached at its end or along its length to a microtubule (that is, at the junction of three-way branch-points in the ER network), it behaved differently. In this case, if the microtubule depolymerized, the ER network did not retract with the microtubule, but continued to undergo slow retrograde flow without attachment to a microtubule. These results show that under normal circumstances, when ER tubules are under centripetal elastic tension, they require attachment to microtubules to undergo slow retrograde flow, but the ER network as a whole can also be moved by actomyosin-based retrograde flow in the absence of microtubules.

New ER tubules form either by a plus-end sliding mechanism or by TACs

To determine whether the initial extension of new tubules from out of the ER network towards the cell periphery occurred by TACs or the sliding mechanism, we examined enlarged time-lapse series of color overlays of individual ER–microtubule interactions as movies. In Figure 2b, at time 0:00, the ER tubule (arrow) had just begun to extend from the polygonal network along the lattice of the microtubule whose tip is marked with an arrowhead. Between time 0:00–3:02, the microtubule plus end did not grow or shorten. During this time, the ER tubule extended by sliding towards the plus end of the microtubule, and by time 2:06, the ER tubule had 'caught up' with the microtubule tip. The ER tubule and microtubule then both extended simultaneously (time 3:02–3:30), shortened simultaneously (time 3:30–3:58), and at time 3:58, the microtubule switched from shortening back to growth whereas the ER tubule continued to shorten, appearing to 'slip' back at 5–10 μm/min velocities, with frequent pauses, along the lattice of the growing microtubule, and coalesce into the ER network (data not shown). This uneven retraction gave the impression that the ER tubule had few sites of attachment to the microtubule, which detached consecutively as it retracted. The positions of the microtubule tip and the ER tubule tip were tracked over time, and the distance between the tips over time was plotted (Figure 2e), clearly illustrating that the ER tubule was formed by sliding along the lattice of a dynamic microtubule, and then undergoing colinear extension and retraction with the growing and shortening microtubule end.

A second example of an ER–microtubule interaction from a different cell illustrating how ER membrane tubules can form by a TAC-driven mechanism is shown in Figure 2d. At time 0:00, a growing microtubule end contacted a thickened region of the ER network (arrowhead). When the microtubule grew further (time 0:00–2:00), the thickened membrane region formed an attachment to the growing microtubule plus end, and a new ER tubule extended from the thickened region simultaneously with the growing microtubule end for several microns. At time 2:00, when the microtubule switched from growth to

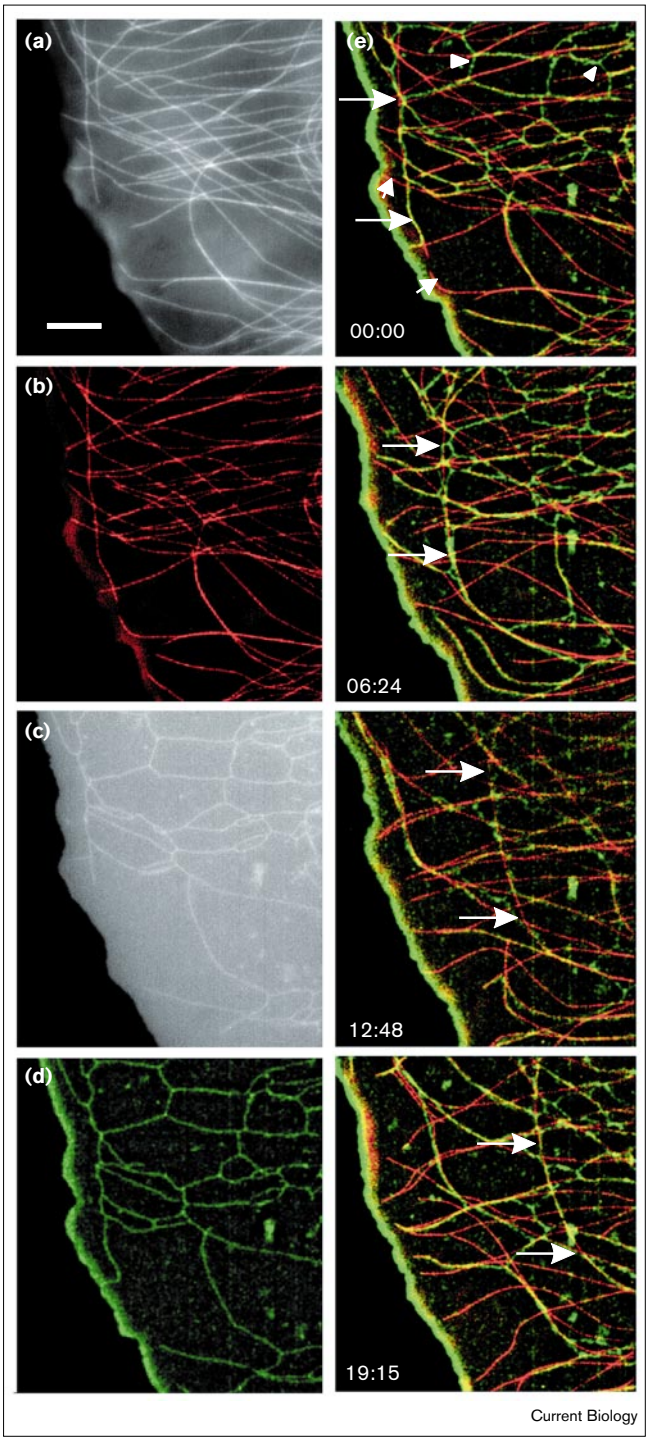

Figure 1

Simultaneous labeling of microtubules with microinjected X-rhodamine-labeled tubulin and ER by $DiOC_6(3)$ staining in the lamella of a living migrating newt lung epithelial cell. The unprocessed images of **(a)** microtubules and **(c)** ER were processed and contrast-enhanced to bring out details of the filamentous and tubular networks against background staining of unpolymerized labeled tubulin and the plasma membrane. The images were then color-coded with **(b)** microtubules red and **(d)** ER tubules green. Note that the image-processing regime used on the ER network artifactually enhances the edge of the cell with brighter staining and makes both ER and microtubules appear more punctate – compare (a,c) with (b,d). **(e)** Processed images of the red microtubules and green ER tubules that were acquired within 3 sec of each other are superimposed into a color overlay to show the relationship of the two structures to each other, and several images from a time-lapse sequence are shown. Arrowheads show regions of the ER network that do not overlie microtubules. Small arrows point to microtubules that do not have ER tubules associated with them. Large arrows point to a microtubule with its associated ER tubule that is parallel to the leading edge of the cell and undergoes a continuous retrograde flow towards the cell center. Elapsed time is indicated at bottom left (in min:sec). Scale bar in (a) = 5 μm.

Figure 2

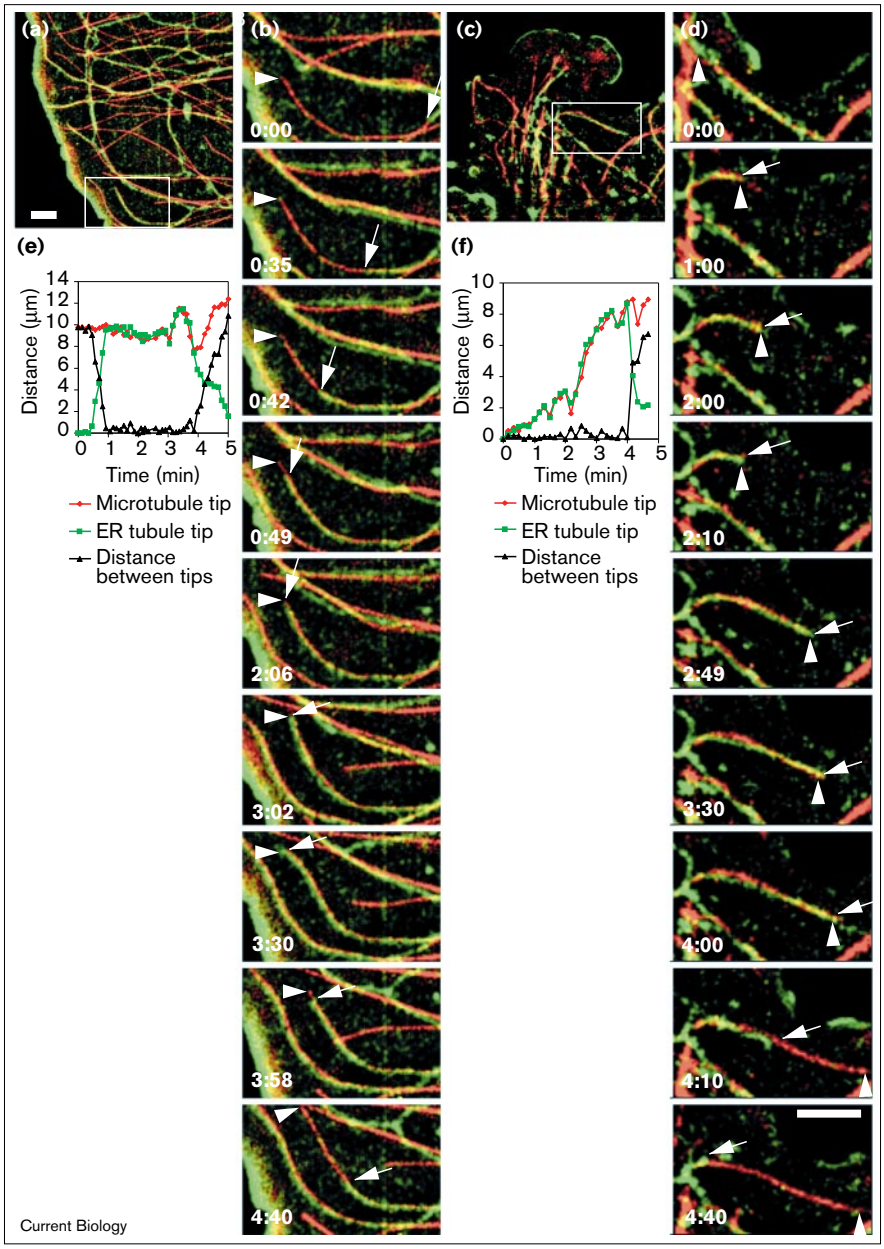

Microtubule-based extension of ER tubules occurs by the sliding mechanism and by TACs. **(a,c)** Processed still color-overlay images from time-lapse sequences of the lamellae of two different cells injected with X-rhodamine-labeled tubulin (red) and stained with $DiOC_6(3)$ (green) are shown at the same magnification (scale bar in (a) is 5 μm). The specific ER–microtubule interactions are highlighted by a white box, and are enlarged to the same magnification in **(b,d)**; scale bar in (d) is 5 μm; elapsed time is shown at the lower left of each panel in min:sec). In (b), an ER tubule (arrow) forms by extending along the lattice of a microtubule (tip marked with arrowhead) from time 0:00–2:06. At 2:06, the tip of the ER tubule has caught up with the tip of the microtubule, and, between time 3:02–3:58, they undergo colinear growth and shortening. Between time 3:58–4:40, the ER tubule retracts along the microtubule lattice while the microtubule switches back to growth. In (d), a microtubule end (arrowhead) contacts a thickened ER region, and as the microtubule grows the ER tubule is extended colinearly (0:00–2:00). The microtubule and ER tubule undergo colinear shortening and growth (2:00–4:00) until the ER tubule suddenly detaches from the microtubule end and recoils (4:10–4:40). **(e,f)** The distance of the microtubule tip and the ER tubule tip (relative to the position of the membrane tubule tip at time 0:00) plotted against time. Also plotted is the distance between the two tips against time. Panel e shows data for formation of ER tubules by sliding towards the plus ends of microtubules; panel f shows data for formation of new ER tubules by coupling to polymerizing microtubule plus ends.

shortening, the ER tubule retracted colinearly with the microtubule tip. The ER tubule and microtubule both shortened for about 1 μm, and both switched to growth (time 2:10) for several microns. At times 3:30 and 4:00, note that the ER tubule is not associated with the microtubule all along its length, but appears to be stretched from its attachment point at the microtubule tip. Just after time 4:00, the ER tubule abruptly lost its attachment to the microtubule tip and rapidly recoiled at 42.3 μm/min (time 4:10) as the microtubule continued to grow. The rapid recoil of the ER tubule indicated that there was only a single point of attachment between the ER tubule and the microtubule end. Plots of the position of the ER tubule tip, microtubule tip, and distance between the two tips over time (Figure 2f) clearly illustrate that the ER membrane tubule was initially formed by coupling to the polymerizing plus end during ER tubule extension, and that the ER tubule remained attached to the plus end during switching between polymerization and depolymerization, and during depolymerization.

The interactions between 75 ER tubules and microtubules were examined in 138 minutes of time-lapse color overlays of a 900 μm^2 field of view of the lamella in 15 different

cells. Of the ER tubules observed, 10.7% were statically attached at their ends to the lattice of microtubules and undergoing retrograde flow, whereas 89.3% were observed to interact dynamically with microtubules (Figure 3). We classified TAC-driven ER tubule formation as an ER tubule that extended *de novo* by its attachment to the tip of a polymerizing microtubule, and the sliding mechanism was classified as an ER tubule that extended *de novo* along the lattice of a pre-existing microtubule, regardless of the assembly state of the microtubule end (see Materials and methods). New ER tubules were formed by the TAC-driven mechanism 31.4% of the time, and by the sliding mechanism 68.6% of the time (Figure 3). ER tubules extended by sliding at an average rate of 4.23 ± 4.64 μm/min (range = 0.21–36.6 μm/min) (Table 1) at a frequency of 0.332 tubules per minute (Figure 3), whereas TACs extended at an average of 3.79 ± 3.46 μm/min (range = 0.30–12.6 μm/min) at a frequency of 0.151 tubules per minute (Table 1). Following their initial formation, ER tubules formed by TACs remained attached to the ends of microtubules during all phases of microtubule dynamic instability. TACs were most likely to detach from microtubule ends during switching from shortening to growth (87% of the time), during growth (10% of the time), or during pause (3% of the time). When sliding ER tubules caught up with the plus ends of microtubules, 88.8% of the time their movement became coupled to the growth and shortening dynamics of the microtubule, presumably forming TACs at that time. The remaining 11.2% of the time, sliding ER remained associated with the microtubule end only very briefly (< 10 seconds) before detaching and retracting along the microtubule lattice. Following microtubule detachment, ER tubules retracted towards the cell center only far enough to coalesce into the ER network and never continued moving beyond this point in a minus-end direction, indicating that retraction was due to centripetal tension in the ER tubule and not minus-end motor activity.

Figure 3

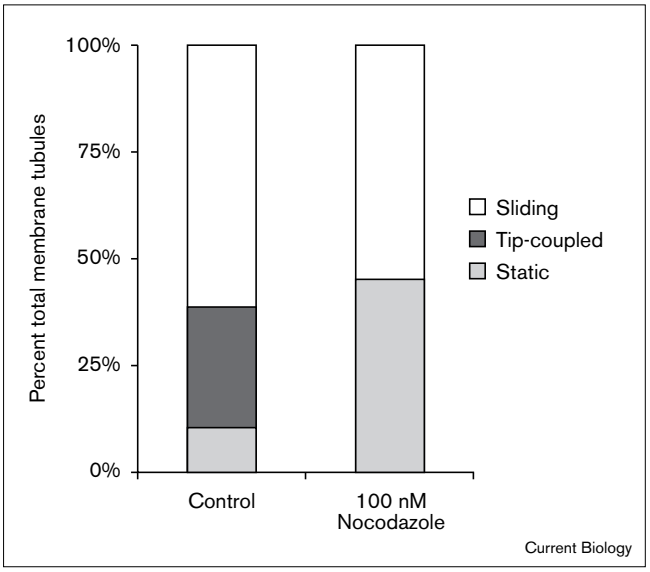

Comparison of the types of interactions between ER tubules and microtubules in control cells and cells treated with 100 nM nocodazole to inhibit microtubule plus-end dynamic instability. Nocodazole (100 nm) selectively inhibited all the TAC motility and increased the percentage of ER tubules that were statically bound to the microtubule lattice. For control, $n = 15$ cells, 138 min; for 100 nM nocodazole, $n = 7$ cells, 70 min. Total tubules observed: control = 0.542 per min, nocodazole = 0.573 per min. Static tubules observed: control = 0.058 per min, nocodazole = 0.258 per min. Dynamic tubules observed: control = 0.484 per min, nocodazole = 0.314 per min. TACs observed: control = 0.152 per min, nocodazole = 0.000 per min. Sliding tubules observed: control = 0.332 per min, nocodazole = 0.314 per min.

TACs do not change microtubule growth and shortening rates but alter transition frequencies

To determine whether TACs alter microtubule growth and shortening kinetics *in vivo*, we compared the parameters of microtubule dynamic instability of microtubules that had no ER associated with their plus end (free plus ends) with those of ER–microtubule TACs (Table 1). Free plus ends had an average growth velocity of 3.65 ± 3.20 μm/min, not significantly different from the 3.79 ± 3.46 μm/min rate of TACs (Table 1). Similarly, the rates of shortening for free plus ends (3.57 ± 3.11 μm/min) and TACs (3.11 ± 3.73 μm/min) were not significantly different. However, the frequency of catastrophe for TACs

Table 1

Parameters of microtubule and ER dynamics.

Plus-end parameter	Free plus ends ($n = 63$)	TACs ($n = 30$)	Sliding ER tubule ($n = 30$)
Elongation rate (μm/min)	3.65 ± 3.20	3.79 ± 3.46	4.23 ± 4.64
Elongation duration (min)	0.38 ± 0.24	0.40 ± 0.26	0.37 ± 0.29
Shortening rate (μm/min)	3.57 ± 3.11	3.11 ± 3.73	3.54 ± 3.64
Shortening duration (min)	0.33 ± 0.21	0.33 ±3.73	0.32 ± 0.13
Catastrophe frequency* (per min)	4.60 ± 3.03	2.24 ± 0.97†	
Rescue frequency* (per min)	5.90 ± 3.82	4.00 ± 2.41†	

Comparison of parameters of microtubule plus-end dynamic instability of free plus ends, and those of microtubules with ER TACs coupled to their plus ends. Also shown are rates and durations of elongation and retraction for ER tubules that are moving by sliding along the lattice of a microtubule. Ten cells were analyzed in all cases, and n is the number of microtubule plus ends or ER tubule tips analyzed. Values are expressed as mean ± SD. *Measured per individual microtubule. †Significantly different from free microtubule, $p < 0.01$.

was significantly reduced ($p < 0.01$) compared with free plus ends: 4.60 ± 3.03 per minute for free plus ends versus 2.24 ± 0.97 per minute for TACs (Table 1). Likewise, the rescue frequency was also significantly reduced by attachment of a TAC to a microtubule tip: 5.90 ± 3.82 per minute for free plus ends versus 4.00 ± 2.41 per minute for TACs (Table 1).

TAC formation requires plus end microtubule assembly and disassembly dynamics

To determine whether microtubule growth and shortening dynamics were required to maintain the ER tubule TAC at a microtubule plus end, cells were treated with a concentration of nocodazole (100 nM) that inhibits plus-end growth and shortening [32,34]. Under these conditions, the inhibited plus ends (Figure 4, arrowheads) moved with retrograde flow towards the cell center. Strikingly, no ER tubules were attached to the ends of microtubules. In contrast, ER tubules continued to form by the sliding mechanism at the normal ER sliding velocity (Figure 4, arrows). Unlike control cells, when sliding ER tubules 'caught up' with stable microtubule plus ends, the ER tubules did not form TACs, but instead associated with the microtubule ends briefly (< 10 seconds) before detaching and retracting along the microtubule lattice (data not shown).

To quantitate the effects of inhibiting microtubule dynamics on ER motility, 40 ER–microtubule interactions were examined in 70 minutes of time-lapse color overlays of a 900 μm^2 field of view of the lamellae of seven different 100 nM nocodazole-treated cells. Not a single ER tubule was coupled to the stable end of a microtubule in nocodazole-treated cells. Although the total number of ER tubules after nocodazole treatment was similar to controls (0.573 per minute versus 0.542 per minute, respectively), the proportion of ER tubules that were statically bound to microtubules was increased from 10.7% in control cells to 45.0% in nocodazole-treated cells (0.058 per minute versus 0.258 per minute, respectively; Figure 3). However, a similar proportion of the total ER tubules were formed by the sliding mechanism in nocodazole-treated and control cells (54.8% versus 61.2%, respectively).

Discussion

Three modes of ER transport in the lamella of migrating cells

We have analyzed the dynamic relationship between ER tubules and microtubules in the peripheral lamella of living migrating newt lung epithelial cells and find evidence for three modes of microtubule-associated ER transport, clearly resolving speculations on this issue that have gone on for many years. ER tubules formed and extended from the reticular network towards the leading edge either by forming a sliding attachment that moved toward the plus end of a microtubule (sliding mechanism) or by attaching to the polymerizing plus end of a microtubule (TAC mechanism). Nocodazole perfusion experiments showed that it was possible for the ER network to undergo retrograde flow when not attached to microtubules. Under normal circumstances, however, the ER is attached to microtubules in the lamella and moves toward the cell center with the actomyosin-driven retrograde flow of microtubules. Thus, the ER is turned over in the lamella by advancement of new tubules towards the periphery by plus-end-directed membrane sliding and TAC mechanisms and is removed by actomyosin-based retrograde flow driving the microtubule movement mechanism. There was no evidence for minus-end-directed sliding of ER in the lamella, but it is possible that minus-end-directed motors may move ER in central regions of these cells or may predominate in centripetal transport in non-motile cells. In contrast, the TAC and sliding mechanisms of ER tubule formation may be ubiquitous phenomena and contribute to many forms of membrane trafficking in the central vacuolar system of the cell.

Why has the cell evolved two distinct mechanisms for forming ER tubules in cells? The mechanisms may be redundant, and in regions of the cells where ER networks

Figure 4

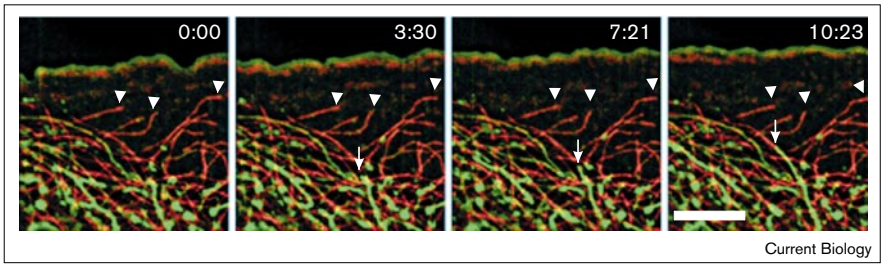

ER and microtubule dynamics in the lamella of a cell treated with low levels of nocodazole to inhibit microtubule dynamic instability. Cells were microinjected with X-rhodamine-labeled tubulin to label microtubules (red), stained with $DiOC_6(3)$ (green) to label ER, and treated with 100 nM nocodazole for ~5 min before a time-lapse series of images was obtained. The microtubule plus ends did not exhibit growth and shortening dynamics and had no ER tubules attached to their plus ends (arrowheads). ER tubules (one highlighted by the arrow), however, still extended in a plus-end direction by sliding along the lattice of microtubules. Note that the leading edge of the cell advanced during the sequence, increasing the distance between the microtubule ends and the edge. Scale bar = 10 μm; time is in min:sec.

are dense and microtubule plus ends are abundant, the TAC mechanism dominates, whereas in regions of the cell that have aligned polarized microtubules and microtubule shafts are abundant, the sliding mechanism predominates. Thus, extension of ER after cell division [31] could utilize TACs, whereas axonal transport of ER [35] may utilize the sliding mechanism. If, as discussed below, both TACs and the sliding mechanism share the same molecules, TACs may form when a microtubule plus end happens to contact a region of the ER where these molecules are located, while a sliding attachment may form if this same ER region contacts the shaft of a microtubule. Subdomains of the ER membrane may concentrate these components. Consistent with this is our observation that both TACs and sliding ER tubules had only one or very few attachment sites to microtubules. Concentration of proteins into functionally distinct subdomains seems to be a general feature of membrane networks, exemplified by ER 'exit sites' where newly synthesized proteins collect prior to their transport to the Golgi [36–38] and motile sites of attachment of Golgi membranes to microtubules where secretory products concentrate [19]. However, because attachment of TACs to microtubules was found to stabilize the microtubule to transitions between growth and shortening, it is also possible that TACs do not serve a transport purpose, but are for modulation of microtubule dynamics.

ER TACs and ER sliding may both share the same molecular complex that includes a kinesin-related protein

We suggest that both sliding and TAC-driven ER movements involve a single molecular complex. This is supported by two observations. First, ER–microtubule TACs in *Xenopus* extracts, ER–microtubule end-attachment sites in growth cones [13], and motile sites of membrane attachment to microtubules [19] all involve similar bulbous membrane structures. Second, ER tubules sliding in a plus-end direction on microtubules often immediately formed TACs when they reached the microtubule tip. This is similar to the behavior of kinesin-coated beads *in vitro*, which in the presence of ATP under certain salt conditions can slide towards the plus end of a depolymerizing microtubule, and upon reaching the depolymerizing end, become coupled to the minus-end-directed movement of microtubule shortening [28]. This suggests that kinesin or a related protein may be a member of the complex. This is supported by experiments in astrocytes and neurons, where inhibition of kinesin with antisense oligonucleotides caused retraction of ER from the cell periphery [39], suggesting that both TACs and sliding movements were inhibited by this single treatment. Because the plus-end-directed sliding rate of ER was surprisingly slow (about 4 μm/min), a kinesin-related protein and probably not conventional kinesin (about 60 μm/min) may be part of the complex. However, ER–microtubule TACs remained attached irrespective of whether the microtubule was growing or shortening. Thus far, *in vitro* coupling of kinesin-coated beads has been documented only for shortening microtubules, and not for growing microtubules, suggesting that other molecules besides kinesins may be members of the complex. Some interesting candidate proteins that have been localized to microtubule ends include XKCM-1, a *Xenopus* kinesin-related protein that induces microtubule catastrophe [40], CLIP-170, a putative endosome–microtubule-linking protein [41], and cytoplasmic dynein, a minus-end-directed microtubule motor [42]. Identification of multifunctional ER motility molecules awaits further investigation.

Conclusions

On the basis of *in vitro* studies of microtubule motor protein motility and recent studies of microtubule motors in membrane trafficking in the cell, a prevailing view has evolved in which ER movement is driven by motor proteins sliding membranes along the shafts of microtubules. We have demonstrated in living cells that ER tubules were extended by microtubules using a combination of the membrane sliding mechanism and a mode that is driven by microtubule plus-end polymerization dynamics, the TAC. ER removal from the lamella was not powered by minus-end-directed motors, but by actomyosin-based retrograde flow. Because ER sliding to microtubule plus ends resulted in TAC formation, membrane sliding and TACs may share the same molecules, most likely including a kinesin. We also found that ER is capable of modulating microtubule assembly dynamics via TACs. The two modes of microtubule-based ER tubule extension may represent redundancy in an important biological function, or could be specialized to specific situations such as the re-spreading of membrane networks after cell division or axonal transport.

Materials and methods

Experimental manipulations

Primary cultures of newt (*Taricha granulosa*) lung epithelial cells were established as described by Reider and Hard [43]. Tubulin was purified from pig brains and was covalently conjugated to X-rhodamine by the method of Hyman *et al.* [44]. The dye:protein ratio was 1.25:1. Cells were microinjected with 2 mg/ml X-rhodamine-labeled tubulin in injection buffer (50 mM potassium glutamate, 0.5 mM KCl, pH = 7.0) as described [32]. Cells were vitally labeled at room temperature for 7 min by addition of 1.5 μg/ml $DiOC_6(3)$ to the culture media as described [31]. Cells were rinsed and mounted on a slide in media containing 30 u/ml Oxyrase (Oxyrase Inc.) [31].

Image acquisition and processing

Pairs of images of X-rhodamine-labeled microtubules and $DiOC_6(3)$-labeled ER were acquired at 7–10 sec intervals using the multi-mode digital imaging system described [32,45]. Briefly, this consisted of epi-illumination from an HBO 100 W mercury arc lamp passed through a heat-reflecting filter, a bandpass filter for either 490 ± 20 nm (for $DiOC_6(3)$) or 570 ± 20 nm (for X-rhodamine), and a neutral density filter before reflecting off of a triple bandpass dichromatic mirror and being focussed onto the specimen via a 60× 1.4 NA DIC objective lens. Illumination wavelength and intensity were selected by a dual filterwheel and shutter apparatus (Metaltek) under the control of MetaMorph software (Universal Imaging). Emission from the specimen was

collected by the objective lens, passed through a triple bandpass emission filter, and magnified 1.875× onto a Hamammatsu C4880 cooled CCD. Camera exposure and shutter controls were also under the control of MetaMorph software.

To examine the relation between membrane tubules and microtubules, color-encoded overlays were created using functions in MetaMorph. For images of both microtubules and ER, the background was subtracted and the contrast stretched to the 12-bit grayscale (4095 levels). A 25×25 kernel size low pass filter was applied to the image, and this was subtracted from the unfiltered image to 'flatten' the field shading and bring out details. The contrast was stretched again to produce the final processed image. The final processed images of microtubules and ER were combined to create a 24-bit RGB color overlay image. These procedures were repeated for all image pairs in a time-lapse series. Movies of time-lapse series of color overlays were made using Adobe Premeir™ as described [46].

Data analysis

Parameters of microtubule dynamic instability were determined as described in [32]. Similar analysis was performed on membrane tubules that extended *de novo* from the ER network. All values are expressed as mean ± SD. To discriminate between the 'sliding' and TAC mechanisms of new ER tubule formation, two criteria were considered. First, movies of microtubule and ER dynamics were examined. If an ER tubule obviously extended along the lattice towards the plus end of a pre-existing microtubule as it was extended from the ER network, it was scored as a 'sliding interaction'; it did not matter whether the microtubule was growing or shortening at the time of the interaction. If the new ER tubule appeared to extend by attachment to the end of a growing microtubule, the following quantitative regime was considered. The positions of both the microtubule and its associated ER tubule were tracked in the unprocessed images. The distance between the ends of the microtubule and membrane tubule tips were calculated and plotted against time. If the distance between the tips was less than 1.5 μm throughout the extension period, they were considered to be a TAC. The distance 1.5 μm was chosen because our resolution of tracking was ± 0.5 μm [32], and the images were acquired within 3 sec of each other, and at the maximal rates of ER tubule movement measured (36 μm/min), the membrane and microtubule tips could be positionally staggered by about 1 μm. The quantitative analysis of unprocessed images was always found to be in agreement with the visual analysis of morphological criteria in processed color overlays, indicating that the image-processing regime did not degrade the positional information in the images.

Supplementary material

Quicktime movies of the time-lapse sequences shown in Figures 1e, 2b, 2d and 4 are published with this paper on the internet.

Acknowledgements

We thank Salmon lab members Jennifer Waters and Paul Maddox for support, Mark Nguyen for help with data analysis, Sid Shaw of Stanford University for suggestions on image processing, Nea Gliksman of Universal Imaging Inc. for help with modifying RTM for use with MetaMorph. This work was supported by NIH GM 24364 to E.D.S. and a fellowship from the Jane Coffin Childs Memorial Fund for Cancer Research to C.M.W-S.

References

1. Buckley IK, Porter KR: **Electron microscopy of critical point dried whole cultured cells.** *J Microsc* 1975, **104:**107-120.
2. Lippincott-Schwartz J, Yuan L, Tipper C, Amherdt M, Orci L, Klausner R: **Brefeldin A's effects on endosomes, lysosomes, and the TGN suggest a general mechanism for regulating organelle structure and membrane traffic.** *Cell* 1991, **67:**601-616.
3. Terasaki M, Song J, Wong JR, Weiss MJ, Chen LB: **Localization of endoplasmic reticulum in living and glutaraldehyde-fixed cells with fluorescent dyes.** *Cell* 1984, **38:**101-108.
4. Lee C, Chen LB: **Behavior of endoplasmic reticulum in living cells.** *Cell* 1988, **54:**37-46.
5. Lee C, Ferguson M, Chen LB: **Construction of the endoplasmic reticulum.** *J Cell Biol* 1989, **109:**2045-2055.
6. Cooper MS, Cornell-Bell AH, Chernjavsky A, Dani JW, Smith SJ: **Tubulovesicular processes emerge from trans-Golgi cisternae, extend along microtubules, and interlink adjacent trans-Golgi elements into a reticulum.** *Cell* 1990, **61:**135-145.
7. Sciaky N, Presley J, Smith C, Zaal KJM, Cole N, Moriera JE, *et al.*: **Golgi tubule traffic and the effects of brefeldin A visualized in living cells.** *J Cell Biol* 1997, **139:**1137-1155.
8. Presley JF, Cole NB, Schroer TA, Hirschberg K, Zaal KJ, Lippincott-Schwartz J: **ER-to-Golgi transport visualized in living cells.** *Nature* 1997, **389:**81-85.
9. Cole NB, Lippincott-Schwartz J: **Organization of organelles and membrane traffic by microtubules.** *Curr Opin Cell Biol* 1995, **7:**55-64.
10. Terasaki M: **Recent progress on structural interactions of the endoplasmic reticulum.** *Cell Motil Cytoskel* 1990, **15:**71-75.
11. Terasaki M, Chen LB, Fujiwara K: **Microtubules and the endoplasmic reticulum are highly interdependent structures.** *J Cell Biol* 1986, **103:**1557-1568.
12. Dailey ME, Bridgman PC: **Dynamics of the endoplasmic reticulum and other membranous organelles in growth cones of cultured neurons.** *J Neurosci* 1989, **9:**1897-1909.
13. Dailey ME, Bridgman PC: **Structure and organization of membrane organelles along distal microtubule segments in growth cones.** *J Neurosci Res* 1991, **30:**242-258.
14. Lippincott-Schwartz J, Cole NB, Marotta A, Conrad PA, Bloom GS: **Kinesin is the motor for microtubule-mediated Golgi-to-ER membrane traffic.** *J Cell Biol* 1995, **128:**293-306.
15. Vaisberg EA, Grissom PM, McIntosh JR: **Mammalian cells express three distinct dynein heavy chains that are localized to different cytoplasmic organelles.** *J Cell Biol* 1996, **133:**831-842.
16. Burkhardt JK, Echeverri CJ, Nilsson T, Vallee RB: **Overexpression of the dynamitin (p50) subunit of the dynactin complex disrupts dynein-dependent maintenance of membrane organelle distribution.** *J Cell Biol* 1997, **139:**469-484.
17. Corthesy-Theulaz I, Pauloin A, Pfeffer SR: **Cytoplasmic dynein participates in the centrosomal localization of the Golgi complex.** *J Cell Biol* 1992, **118:**1333-1345.
18. Sheetz MP: **Microtubule motor complexes moving membranous organelles.** *Cell Struct Func* 1996, **21:**369-373.
19. Allan V, Vale R: **Movement of membrane tubules along microtubules *in vitro*: evidence for specialised sites of motor attachment.** *J Cell Sci* 1994, **107:**1885-1897.
20. Allan VJ, Vale RD: **Cell cycle control of microtubule-based membrane transport and tubule formation *in vitro*.** *J Cell Biol* 1991, **113:**347-359.
21. Schroer TA, Sheetz MP: **Two activators of microtubule-based vesicle transport.** *J Cell Biol* 1991, **115:**1309-1318.
22. Dabora SL, Sheetz MP: **The microtubule-dependent formation of a tubulovesicular network with characteristics of the ER from cultured cell extracts.** *Cell* 1988, **54:**27-35.
23. Vale RD, Hotani H: **Formation of membrane networks *in vitro* by kinesin-driven microtubule movement.** *J Cell Biol* 1988, **107:**2233-2241.
24. Waterman-Storer CM, Gregory J, Parsons SF, Salmon ED: **Membrane/microtubule tip attachment complexes (TACs) allow the assembly dynamics of plus ends to push and pull membranes into tubulovesicular networks in interphase *Xenopus* egg extracts.** *J Cell Biol* 1995, **130:**1161-1169.
25. Reinsch S, Karsenti E: **Movement of nuclei along microtubules in *Xenopus* egg extracts.** *Curr Biol* 1997, **7:**211-214.
26. Blocker A, Griffiths G, Olivo J-C, Hyman AA, Severin FF: **A role for microtubule dynamics in phagosome movement.** *J Cell Sci* 1998, **111:**303-312.
27. Coue M, Lombillo VA, McIntosh JR: **Microtubule depolymerization promotes particle and chromosome movement *in vitro*.** *J Cell Biol* 1991, **112:**1165-1175.
28. Lombillo VA, Stewart RJ, McIntosh JR: **Minus-end-directed motion of kinesin-coated microspheres driven by microtubule depolymerization.** *Nature* 1995, **373:**161-164.
29. Lombillo VA, Nislow C, Yen TJ, Gelfand VI, McIntosh JR: **Antibodies to the kinesin motor domain and CENP-E inhibit microtubule depolymerization-dependent motion of chromosomes *in vitro*.** *J Cell Biol* 1995, **128:**107-115.
30. Terasaki M, Reese TS: **Interactions among endoplasmic reticulum, microtubules, and retrograde movements of the cell surface.** *Cell Motil Cytoskel* 1994, **29:**291-300.

31. Waterman-Storer CM, Sanger JW, Sanger JM: **Dynamics of organelles in the mitotic spindles of living cells: membrane and microtubule interactions.** *Cell Motil Cytoskel* 1993, **26:**19-39.
32. Waterman-Storer CM, Salmon ED: **Actomyosin-based retrograde flow of microtubules in the lamella of migrating epithelial cells influences microtubule dynamic instability and turnover and is associated with microtubule breakage and treadmilling.** *J Cell Biol* 1997, **139:**417-434.
33. Cramer LP, Mitchison TJ: **Myosin is involved in postmitotic cell spreading.** *J Cell Biol* 1995, **131:**179-189.
34. Vasquez RJ, Howell B, Yvon AM, Wadsworth P, Cassimeris L: **Nanomolar concentrations of nocodazole alter microtubule dynamic instability *in vivo* and *in vitro*.** *Mol Biol Cell* 1997, **8:**973-985.
35. Terasaki M, Slater NT, Fein A, Schmidek A, Reese TS: **Continuous network of endoplasmic reticulum in cerebellar Purkinje neurons.** *Proc Natl Acad Sci USA* 1994, **91:**7510-7514.
36. Saraste J, Svensson K: **Distribution of the intermediate elements operating in ER to Golgi transport.** *J Cell Sci* 1991, **100:**415-430.
37. Plutner H, Davidson HW, Saraste J, Balch WE: **Morphological analysis of protein transport from the ER to Golgi membranes in digitonin-permeabilized cells: role of the P58 containing compartment.** *J Cell Biol* 1992, **119:**1097-1116.
38. Cole NB, Sciaky N, Marotta A, Song J, Lippincott-Schwartz J: **Golgi dispersal during microtubule disruption: regeneration of Golgi stacks at peripheral endoplasmic reticulum exit sites.** *Mol Biol Cell* 1996, **7:**631-650.
39. Feiguin F, Ferreira A, Kosik KS, Caceres A: **Kinesin-mediated organelle translocation revealed by specific cellular manipulations.** *J Cell Biol* 1994, **127:**1021-1039.
40. Desai A, Mitchison TJ, Walczak CE: **Microtubule destabilization by XKCM1 and XKIF2 – two internal motor domain subfamily kinesins.** *Mol Biol Cell* 1997, **8:**3a.
41. Pierre P, Scheel J, Rickard JE, Kreis TE: **CLIP-170 links endocytic vesicles to microtubules.** *Cell* 1992, **70:**887-900.
42. Vaughn KT, Tynan SH, Faulkner NE, Echeverri CJ, Vallee RB: **Evidence for co-localization with CLIP-170 at microtubule distal ends.** *Mol Biol Cell* 1997, **7:**403a
43. Rieder CL, Hard R: **Newt lung epithelial cells: cultivation, use, and advantages for biomedical research.** *Int Rev Cytol* 1990, **122:**153-220.
44. Hyman A, Drechsel D, Kellogg D, Salser S, Sawin K, Steffen P, *et al.*: **Preparation of modified tubulins.** *Meth Enzymol* 1991, **196:**478-485.
45. Salmon ED, Shaw SL, Waters J, Waterman-Storer CM, Maddox PS, Yeh E, Bloom KA: **High resolution multi-mode digital microscope system.** *Meth Cell Biol* 1998, **56:**185-214.
46. Waterman-Storer CM, Shaw SL, Salmon ED: **Production and presentation of digital movies.** *Trends Cell Biol* 1997, **7:**503-506.

Because *Current Biology* operates a 'Continuous Publication System' for Research Papers, this paper has been published on the internet before being printed. The paper can be accessed from http://biomednet.com/cbiology/cub – for further information, see the explanation on the contents page.

Supplementary material

Endoplasmic reticulum membrane tubules are distributed by microtubules in living cells using three distinct mechanisms

Clare M. Waterman-Storer and E.D. Salmon

Current Biology 12 June 1998, **8:**798–806

Movies

Quicktime movies of the time-lapse sequences shown in Figures 1e, 2b, 2d and 4.